

Electrochemical Characterization of Some Electrode Materials for Pharmaceutically Active Compounds Degradation

A. Remes*, M. Ihos** and F. Manea*

*Politehnica" University of Timisoara, Faculty of Industrial Chemistry and Environmental Engineering,
P-ta Victoriei nr.2, 300006 Timisoara, Romania, e-mail: florica.manea@chim.upt.ro;
adriana.remes@chim.upt.ro

**National Research and Development Institute for Industrial Ecology–ECOIND, Timisoara Branch, P-ta Regina Maria nr.1, 300004
Timisoara, Romania, e-mail: monica.ihos@chim.upt.ro

Abstract. The aim of this paper was the electrochemical characterization of Dimensionally Stable Anodes (DSA), Boron Doped Diamond (BDD) and expanded graphite-silver doped zeolite-epoxy composite (EG-Z-Ag-Epoxi) electrodes for ibuprofen (IBP) electrooxidation. IBP is one of the pharmaceutically active compounds (PhACs) that belongs to anti-inflammatory drugs and has in its structure an aromatic ring. The morphological data regarding the electrode materials were obtained by recording scanning electron microscopy (SEM) images. The electrochemical characterization of the electrode materials was carried out by cyclic voltammetry (CV). The supporting electrolyte in CV experiments was 0.1 M Na₂SO₄. The cyclic voltammograms recorded in the potential range - 0.5 V → + 1.5 V vs. SCE in the presence and absence of IBP revealed that the oxidation process at DSA electrodes and BDD could occur under simultaneous O₂ evolution, and no oxidation peak was evidenced. The voltammetric response of EG-Z-Ag-Epoxi electrode recorded in the potential range - 0.5 V → + 1.25 V vs. SCE showed an oxidation peak before the oxygen evolution and another one in the potential range of oxygen evolution. These findings proved that the oxidation of IBP on the EG-Z-Ag-Epoxi electrode occurred in two steps.

Keywords: Boron-Doped Diamond electrode, Dimensionally Stable Anodes, zeolite modified electrode, cyclic voltammetry, ibuprofen

1. Introduction

The pharmaceutically active compounds (PhACs) are produced and used in very large amounts and their use and diversity is increasing every year [1, 2].

The PhACs are designed to have biological effects but at the same time a great part of the medicines taken by the human beings or animals passes through their bodies unmodified. Also, the fish farms and pharmaceutical manufacturing discharges generate a various range of residuals PhACs that emerge in the environment. Consequently, PhACs emerge the aquatic bodies where they have undesirable effects on aquatic organisms [3].

The PhACs are organic chemicals that are structurally complex and resistant to biological degradation and they are not completely removed in wastewater treatment systems [4,5]. In the recent years, reserches have been conducted to develop effective treatment methods of wastewaters containing PhACs. Thus, it have been reported advanced oxidation processes (UV/H₂O₂, O₃, TiO₂ photocatalysis, photo-Fenton) [6-11] and ultrasonic treatment [12]. Also, electrochemical methods have been applied for removal of antibiotics and salicylic acid from wastewaters [13, 14].

As it is well known, the effectiveness of the electrochemical methods is strongly depend on the choice of the electrode material. The electrochemical characterization of the electrode materials can be carried

out by cyclic voltammetry (CV) that is one of the most frequently used electrochemical methods due to its relative simplicity and very rich informational content [15-17].

The aim of this paper was the electrochemical characterization of the Dimensionally Stable Anodes (DSA), Boron Doped Diamond (BDD) and expanded graphite-silver doped zeolite-epoxy composite (EG-Z-Ag-Epoxi) electrodes during the oxidation of ibuprofen (IBP). IBP is a non-steroidal anti-inflammatory drug and was chosen as model for PhACs because it is considered to be one of the most important contaminats in sewage treatment plant influents.

2. Experimental

2.1. Electrodes preparation

The DSA electrodes, Ti/RuO₂-TiO₂ (molar ratio Ru:Ti in precursors solution 30:70), Ti/IrO₂-TiO₂(molar ratio Ir:Ti in precursors solution 30:70), Ti/RuO₂/SnO₂-Sb₂O₅ (molar ratio Sn:Sb in precursors solution 97:3) and Ti/RuO₂/SnO₂-Sb₂O₅-RuO₂ (molar ratio Sn:Sb:Ru in precursors solution 94:3:3) were obtained by thermal decomposition of the appropriate precursors. Exhaustive description of the electrodes preparation was done previously [18,19].

The BDD electrode was commercially provided by Windsor Scientific Ltd (the United Kingdom).

The EG-Z-Ag-Epoxi (mass ratio EG:Z-Ag=1:2) electrode was obtained by mixing the expanded graphite filler with silver doped zeolite and the epoxy resin. Details were presented in our previous papers [20,21].

2.2. SEM analysis

SEM images of the thin films were obtained by using a Philips CM30T (Netherlands) scanning electron microscope.

2.3. Cyclic voltammetry

The cyclic voltammetric experiments were performed by using an EcoChemie Autolab-PGSTAT 302 (the Netherlands) potentiostat-galvanostat controlled by GPES 4.9 software. DSA, BDD and EG-Z-Ag-Epoxi electrodes with active surface area of 1 cm^2 , 0.071 cm^2 and 0.1962 cm^2 , respectively were working electrodes. A saturated calomel electrode was used as a reference electrode and a platinum plate of 1 cm^2 as a counter electrode. Experiments were carried out at 50 mVs^{-1} scan rates at room temperature in solution of $0.1 \text{ M Na}_2\text{SO}_4$ supporting electrolyte and solutions of IBP of 25 - 100 ppm in $0.1 \text{ M Na}_2\text{SO}_4$.

2.4. Chemicals

IBP is the common name of 2-[4-(2-methylpropyl)phenyl]propanoic acid and it was supplied by BASF (Germany). The chemical structure of IBP is shown in Fig.1. Na_2SO_4 was supplied by Merck (Germany). Distilled water was used for preparing the solutions.

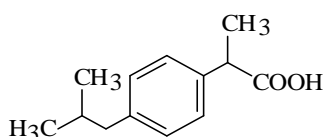


Figure 1. Chemical structure of IBP

3. Results and Discussion

3.1. SEM analysis

The "craked-mud" morphology is typical for the electrodes obtained by thermal decomposition method. The SEM images of DSA electrodes used in the experiments proved this feature (Fig.2) and they are in line with the literature [22].

SEM analysis provided qualitative information about the distribution of expanded graphite and Ag-doped zeolite zones and some surface features of the composite electrode as it is shown in our previous researches [21]. It was observed a closely spaced expanded graphite zones with random distribution and orientation due to the irregular

shapes of both the expanded graphite particles and Ag-modified zeolite particles in epoxy matrix.

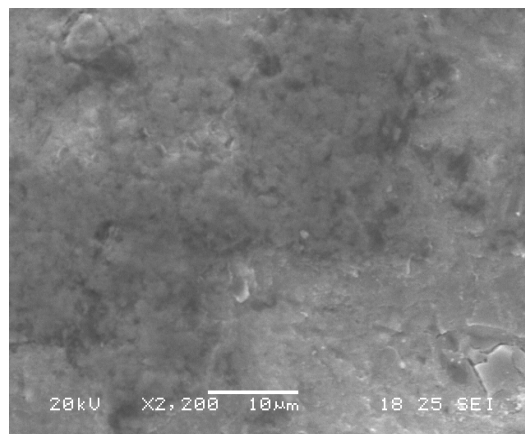


Figure 2. SEM image of Ti/RuO₂/SnO₂-Sb₂O₅; magnification 2200x

3.2. Cyclic voltammetry

The cyclic voltammograms of the studied electrode materials provided relevant information about their electrochemical behaviour during the electrochemical oxidation of IBP and also about the oxygen evolution potential. These informations are very useful to elucidate the IBP electrooxidation mechanism in order to select the electrode material and optimum conditions for the practical applications.

The cyclic voltammograms of DSA electrodes in the potential range from -0.5 V to $+1.5 \text{ V}$ vs. SCE in $0.1 \text{ M Na}_2\text{SO}_4$ supporting electrolyte and in the presence of IBP are shown in Fig. 3-6. The cyclic voltammograms revealed that the oxygen evolution occurred at about $+1.1 \text{ V}$ vs. SCE on the four electrodic compositions of DSA. Below this value of the potential the oxidation current was almost constant and neither anodic nor cathodic peaks were identified. The oxidation current increased sharply above 1.1 V vs. SCE as a result of oxygen evolution.

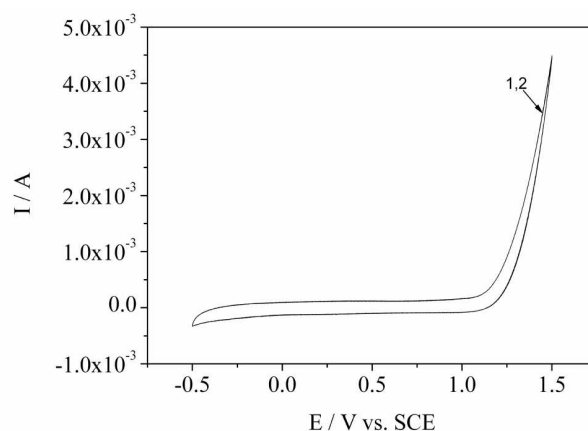


Figure 3. Cyclic voltammograms of Ti/RuO₂-TiO₂; scan rate 0.05 V/s ; potential range: $-0.5 \text{ V} \rightarrow +1.5 \text{ V}$ vs. SCE; 1- $0.1 \text{ M Na}_2\text{SO}_4$; 2- 50 ppm IBP in $0.1 \text{ M Na}_2\text{SO}_4$

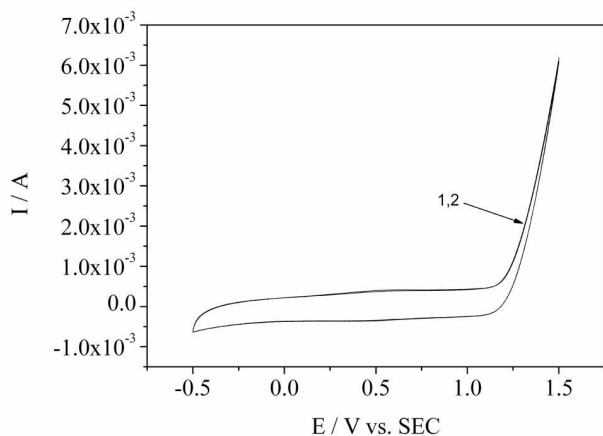


Figure 4. Cyclic voltammograms of Ti/IrO₂-TiO₂; scan rate 0.05 V/s; potential range: -0.5 V → +1.5 V vs. SCE; 1- 0.1 M Na₂SO₄; 2 – 50 ppm IBP in 0.1 M Na₂SO₄

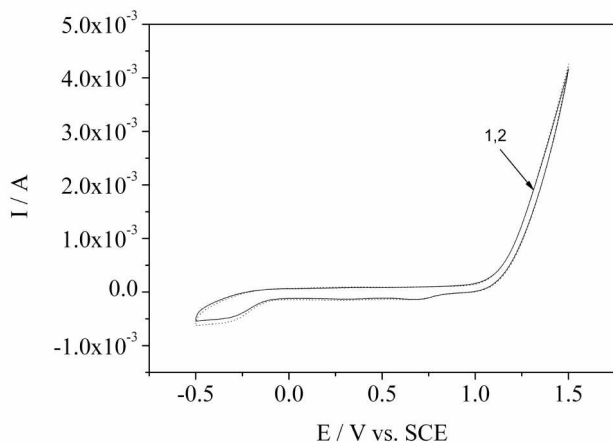


Figure 5. Cyclic voltammograms of Ti/RuO₂/SnO₂-Sb₂O₅; scan rate 0.05 V/s; potential range: -0.5 V → +1.5 V vs. SCE; 1- 0.1 M Na₂SO₄; 2 – 50 ppm IBP in 0.1 M Na₂SO₄

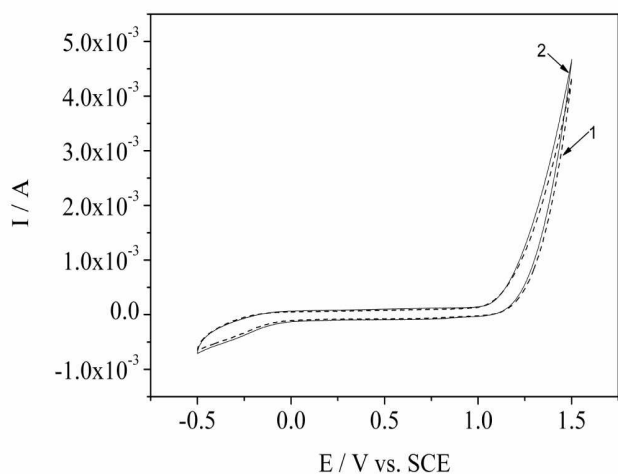


Figure 6. Cyclic voltammograms of Ti/RuO₂/SnO₂-Sb₂O₅-RuO₂; scan rate 0.05 V/s; potential range: -0.5 V → +1.5 V vs. SCE; 1- 0.1 M Na₂SO₄; 2 – 50 ppm IBP in 0.1 M Na₂SO₄

However, an exception for Ti/RuO₂/SnO₂-Sb₂O₅ was recorded. The cyclic voltammogram (Fig.5) showed a cathodic peak at +0.7 V vs. SCE, and in keeping with literature [23], it could be attributed to the reduction process of the intermediate resulted during the oxidation process of the electrode surface under the oxygen potential range.

The same shapes of the voltammograms recorded in the presence and the absence of IBP suggested that no direct oxidation of the IBP on DSA surface occurred, and probably the oxidation process occurred under the simultaneous oxygen evolution [24].

The cyclic voltammogram of BDD electrode recorded in the potential range from -0.5 V to 1.5 V vs. SCE (Fig.7) in the presence and the absence of IBP showed that oxygen evolution potential occurred at about +1.1 V vs. SCE. The rapid increase of the anodic current beyond this value is due to the oxygen evolution. Also, it can be observed that the pollutant oxidation occurred in the potential range of oxygen evolution. However, in comparison with DSA, the anodic current increased in the presence of IBP, even if no oxidation peak corresponding to IBP oxidation process appeared.

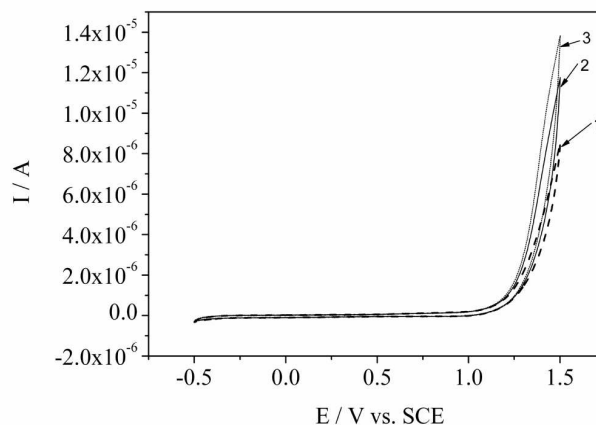


Figure 7. Cyclic voltammograms of BDD electrode in supporting electrolyte 0.1 M Na₂SO₄ and in presence of IBP at various concentration: 1 – 0 ppm; 2- 25 ppm; 3 – 50 ppm; scan rate 0.05 V/s; potential range: -0.5 V → +1.5 V vs. SCE

The cyclic voltammogram of EG-Z-Ag-Epoxy electrode in 0.1 M Na₂SO₄ recorded in the potential range from -0.5 V to +1.25 V vs. SCE (Fig.8) shows two oxidation/reduction peaks corresponding to the redox couples Ag/Ag(I) and Ag(I)/Ag(II). On the anodic curve of the voltammogram the second peak is not well defined because the oxidation process occurred under the simultaneous oxygen evolution that started at +1 V vs. SCE.

The cyclic voltammograms of EG-Z-Ag-Epoxy electrode recorded in the potential range -0.5 V → +1.25 V vs. SCE in the presence and absence of IBP showed that its oxidation occurred in two steps (Fig.9). The oxidation steps are preceded by adsorption step that was evidenced by the decrease of the currents corresponding to Ag/Ag(I) redox couple. As the oxidation process in the potential range until the oxygen evolution exhibits a non-linear dependence (see detail) between the oxidation peak current

and IBP concentrations, the second oxidation step that occurred at +1.18 V vs. SCE, under simultaneous oxygen evolution, exhibited a linear dependence of these parameters. The linear increase of the current with the concentration could be assigned to the increase of the oxidation rate, if the oxidation process is controlled by the mass transfer.

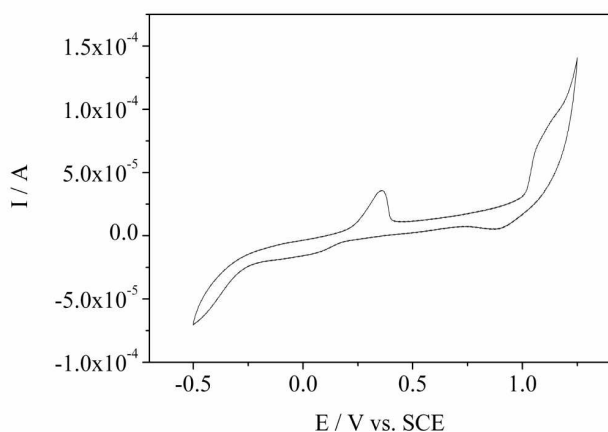


Figure 8. Cyclic voltammogram of EG-Z-Ag-Epoxi electrode (mass ratio EG:Z-Ag=1:2) in 0.1 M Na₂SO₄; scan rate 0.05 V/s; potential range: - 0.5 V → + 1.25 V vs. SCE

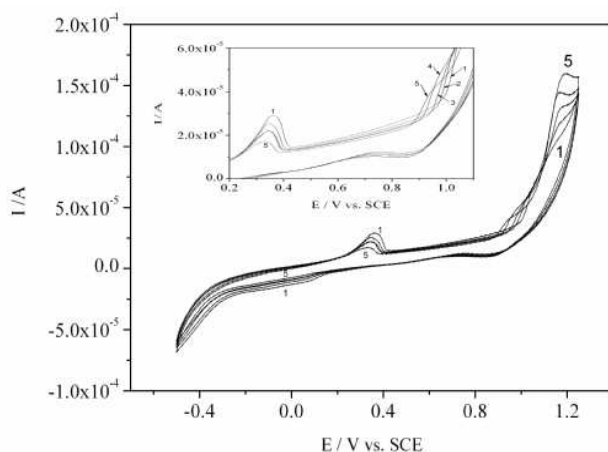


Figure 9. Cyclic voltammograms of EG-Z-Ag-Epoxi electrode, mass ratio EG:Z-Ag=1:1.2 in supporting electrolyte 0.1 M Na₂SO₄ and in presence of IBP at various concentration: 1 – 0 ppm; 2- 25 ppm; 3 – 50 ppm; 4 – 75 ppm; 5 – 100 ppm; scan rate 0.05 V/s; potential range: - 0.5 V → + 1.25 V vs. SCE

4. Conclusions

This paper studied the electrochemical behaviour of DSA, BDD and EG-Z-Ag-Epoxi electrodes during the electrochemical oxidation of IBP, an anti-inflammatory drug. The carried out experiments provided useful information regarding the suitability of these electrode materials to electrochemical degradation of PhACs from pharmaceutical effluents.

Data about the electrode materials morphology were obtained by SEM and revealed the “mud-cracks” surface of DSA and the random distribution and orientation of both

the expanded graphite particles and Ag-modified zeolite particles in epoxy matrix.

Cyclic voltammetry results for all electrode materials studied for IBP oxidation showed that each electrode exhibited a different electrochemical behaviour in the presence of IBP. No changing of the shapes of cyclic voltammograms in the absence and in the presence of IBP was noticed for DSA, and it can be said that the oxidation of IBP could occur under simultaneous oxygen evolution. BDD electrode exhibited the availability for oxidation under water decomposition potential range. CVs recorded for EG-Z-Ag-Epoxi electrode in the same potential range revealed that the oxidation of IBP occurred in two steps, e.g., the first one before the oxygen evolution at about +0.9 V/SCE, and the second one in the potential range of oxygen evolution at +1.18V/SCE. Also, the sorption stage of IBP on Ag/Ag(I) redox couple was noticed.

REFERENCES

1. Bound J.P., and Voulvoulis N., *Chemosphere*, 56, **2004**, 1143-1155.
2. Kummerer K., *J. Environ. Manage.*, 90, **2009**, 2354-2366
3. Enick O.V. and Moore M.M., *Environ. Impact. Asses*, 27, **2007**, 707-729.
4. Kulik N., Trapido M., Goi A., Veressinina Y. and Munter R., *Chemosphere*, 70, **2008**, 1525-1531.
5. Cunningham V.L., Binks S.P. and Olson M.J., *Regul. Toxicol. Pharm.*, 53, **2009**, 39-45.
6. Vogna D., Marotta R., Napolitano A., Andreozzi R. and d'Ischia M., *Water Res.*, 38, **2004**, 414-422.
7. Mendez-Arriaga F., Esplugas S. and Gimenez J., *Water Res.*, 42, **2008**, 585-594.
8. Yang L., Yu L.E. and Ray M.B., *Water Res.*, 42, **2008**, 3480-3488.
9. Cavalheiro A.A., Bruno J.C., Saeki M.J., Valente J.P.S. and Florentino A.O., *Thin Solid Films*, 516, **2008**, 6240-6244.
10. Rizzo L., Meric S., Kassinos D., Guida M., Russo F. and Belgiorno V., *Water Res.*, 43, **2009**, 979-988.
11. Perez-Estrada L.A., Maldonado M.I., Gernjak W., Aguera A., Fernandez-Alba A.R., Ballesteros M.M. and Malato S., *Catal. Today*, 101, **2005**, 219-226.
12. Mendez-Arriaga F., Torres-Palma R.A., Petrier C., Esplugas S., Gimenez J. and Pulgarin C., *Water Res.*, 42, **2008**, 4243-4248.
13. Carlesi Jara C., Fino D., Specchia V., Saracco G. and Spinelli P., *Appl. Catal. B-Environ*, 70, **2007**, 479-487.
14. Guinea E., Arias C., Cabot P.L., Garrido J.A., Rodriguez R.M., Centellas F. and Brillas E., *Water Res.*, 42, **2008**, 499-511.
15. Torriero A.A.J., Tonn C.E., Sereno L. and Raba J., *J. Electroanal. Chem.*, 588, **2006**, 218-225.
16. Bodoki E., Laschi S., Palchetti I., Săndulescu R. and Mascini M., *Talanta*, 76, **2008**, 288-294
17. Hajjizadeh M., Jabbari A., Heli H., Moosavi-Movahedi A.A. and Haghgoo S., *Electrochim. Acta*, 53, **2007**, 1766-1774.
18. Ihos M. and Bocea G., Book of Proceedings of the 3rd International Conference „Ecological Chemistry”, Chisinau, Republic of Moldova, May 20-21, **2005**, 766-772.
19. Ihos M., Manea F., Bocea G. and Jitaru M., *Rev. Roum. Chim.*, 54, **2009**, 301-307.
20. Pop A., Manea F., Radovan C., Malchev P., Bebeselea A., Proca C., Burtica G., Picken S. and Schoonman J., *Electroanal.*, 20, **2008**, 2460-2466.
21. Manea F., Pop A., Radovan C., Malchev P., Bebeselea A., Burtica G., Picken S. and Schoonman J., *Sensors*, 8, **2008**, 5806-5819.
22. Tolba R., Tian M., Wen J., Jiang Z.H. and Chen A., *J. Electroanal. Chem.*, in press.
23. Correa-Lozano B., Comninellis Ch. and Battisti A., *J. Appl. Electrochem.*, 26, **1996**, 683-688.
24. Simond O., Schaller, V. and Comninellis Ch., *Electrochim. Acta*, 42, **1997**, 2009-2012.

Received: 27 May 2010

Accepted: 23 November 2010